We are IntechOpen, the world's leading publisher of Open Access books Built by scientists, for scientists

4,800
Open access books available

122,000
International authors and editors

135M
Downloads

Our authors are among the

154
Countries delivered to

TOP 1%
most cited scientists

12.2%
Contributors from top 500 universities

CLARIVATE ANALYTICS BOOK CITATION INDEX INDEXED

WEB OF SCIENCE™

Selection of our books indexed in the Book Citation Index in Web of Science™ Core Collection (BKCI)

Interested in publishing with us?
Contact book.department@intechopen.com

Numbers displayed above are based on latest data collected.
For more information visit www.intechopen.com

Chapter 11

Quantum Dots Solar Cells

Khalil Ebrahim Jasim

Additional information is available at the end of the chapter

http://dx.doi.org/10.5772/59159

1. Introduction

One of the foremost challenges in solar cells industry is reducing the cost/watt of delivered solar electricity. In conventional microstructures (bulk) single junction solar cells, photons with energies less than semiconductor bandgap are not harvested while those with energies much larger than the bandgap produce hot-carries and upon cooling down (thermalization) the excess energyget wasted as heat. Therefore, novel materials or structures with tunable bandgap or intermediate band that can be tuned to match the spectral distribution of solar spectrum arecrucial. Quantum dots (QDs) have the advantage of tunable bandgap as a result of size variation as well as formation of intermediate bands. In contrast to traditional semiconductor materials that are crystalline or amorphous, quantum dots can be molded into a variety of different types, in two-dimensional (sheets) or three-dimensional arrays. They can be processed to create junctions on inexpensive substrates such as plastics, glass or metal sheets.They can easily be combined with organic polymers and dyes.

Quantum dots are a special class of semiconductors, which are nanocrystals, composed of periodic groups of II-VI, III-V, or IV-VI materials and can confine electrons (quantum confinement). When the size of a QD approaches the size of the material's exciton Bohr radius, quantum confinement effect becomes prominentand electron energy levels can no longer be treated as continuous band, they must be treated as discrete energy levels. Hence, QD can be considered as an artificial molecule with energy gap and energy levels spacing dependent on its size (radius). The energy band gap increases with a decrease in size of the quantum dot, as shown in Figure 4. As the size of a QD increases its absorption peak is red shifted due to shrinkage of its bandgap (see Figure 5). The adjustable bandgap of quantum dots allow the construction of nanostructured solar cell that is able to harvest more of the solar spectrum.QDs have large intrinsic dipole moments, which may lead to rapid charge separation. Quantum dots have been found to emit up to three electrons per photon dueto multiple exciton gener-

ation (MEG), as opposed to only one for standard crystalline silicon solar cell.Theoretically, this could boost solar power efficiencyfrom 20 % to as high as 65 %.

Generally speaking, there are three important parameters that characterize the performance of a photovoltaic cell. These are the open-circuit voltage (V_{oc}), the short circuit current (I_{sc}), and the fill factor ($F\,F$). However, the fill factor is also a function of V_{oc} and I_{sc}. Therefore, these last two parameters are the key factors for determining the cell's power conversion efficiency. Under ideal conditions, each photon incident on the cell with energy greater than the band gap will produce an electron flowing in the external circuit. The fill factor is determined from the maximum area of the I-V characteristics under illumination and the short circuit current and open circuit voltage, or

$$FF = \frac{V_{mp}\ \mathrm{I}_{\mathrm{m}\,p}}{V_{oc}\ I_{sc}} \tag{1}$$

where V_{mp} and I_{mp} are the operating point that will maximize the power output. In this case, the energy conversion efficiency is given by:

$$\eta = \frac{V_{oc}\ \mathrm{I}_{sc}\ FF}{P_{in}} \tag{2}$$

where P_{in} is the input power.

This chapter main objective is to give an introductory coverage of a more sophisticated subject. After we review the physics, designs, structures, and some growth/synthesis techniques of quantum dots. We will give a comprehensive description of some architectures of QD solar cells (e.g., Schottky cell, p-i-n configuration, depleted heterojunction, and quantum dots sensitized solar cell. Also, challenges and opportunities of quantum dots solar cells will be discussed.

2. Brief history of quantum dots

Since the early days of 1960s colloidal semiconductor crystallites or quantum dots concept has been suggested as a new structure of semiconductor materials. In 1981 Ekimove [1] reported the existence of semiconductor crystallitesin a glass matrix. In 1985 Louis Brus developed a quantum model of spherical quantum dots based on effective mass model [2]. Quantum dot term was coined in 1988 by Reed's group [3]. Smith and his coworkers [4] successfully reported the growth of quantum film by depositing 3D silver Ag islands on gallium arsenide GaAs substrate in a two-step process. By the end of the 1990s, commercial productions of colloidal quantum dots becomefeasible. In 2004 a research group at Los Alamos [5] reported that a quantum dotis capable of emitting up to three electrons per photon, as opposed to onlyone for

http://dx.doi.org/10.5772/59159

standard single crystalline layer semiconductors. It is now well established that absorption of high energy photon ($8\times E_g$) quantum dot is capable of generation seven photo-generated charge carriers due to inverse Auger recombination [6]. Now a days quantum dots are promising nanostructure materials in photonics and biomedical applications.

3. Physics of quantum dots

In a bulk semiconductor, electrons and holes are free to move and there is no confinement and hence they have continuous energy values, where energy levels are so close to each other and packed such that energy bands are formed. Occupied bands called valance band and empty ones called conduction bands. The highest occupied band (valance band) and the lowest unoccupied band (conduction band) are separated by what is called energy bandgap E_g. Exciton is formed when electron hole pair are generated. The bond electron-hole system (exciton) form a hydrogen like atom. The separation of between the electron-hole is called Bohr's radius. Table 1 presents examples of exciton Bohr radius for some semiconductors.

Semiconductor Structure	Exciton Bohr Radius (nm)	Bandgap Energy (eV)
PbS	40.0	0.41
GaAs	28.0	1.43
CdTe	15.0	1.50
CdSe	10.6	1.74
ZnSe	8.4	2.58
CdS	5.6	2.53

Table 1. Exciton Bohr radius and bandgap energy of some common semiconductors.

Dimensionality of a material specifies how many dimensions do the carriers of thematerial act as free carriers. In bulk semiconductor continuous density of states results in both conduction and valence bands. However, when the number of atoms in the lattice is very few, the density of states becomes discrete, and loses the continuous 'band' likefeature. Generally speaking, when a material has one or more dimensions small enough to affect itselectronic density of state as illustrated in Figure 1, then the material is said to be confined. Accordingly we can have quantum wells, quantum wires, and quantum dots. Bulk semiconductor materials are example of three dimensional systems where density of states is proportional to $(E-E_{c/v})^{1/2}$. Quantum well system is a two dimensional system where electrons are confined in one dimension and therefore possess step like density of states. Quantum wire system is a one dimensional systemwhere electrons are confined in two dimensions and therefore possess density of states proportional to $(E-E_{c/v})^{-1/2}$. Quantum dot is a zero dimensional system where electron motion is confined in three dimensions. Therefore, a quantum dot possess atomic like density of states that is described mathematically by a delta function $\delta(E-E_{c/v})$.

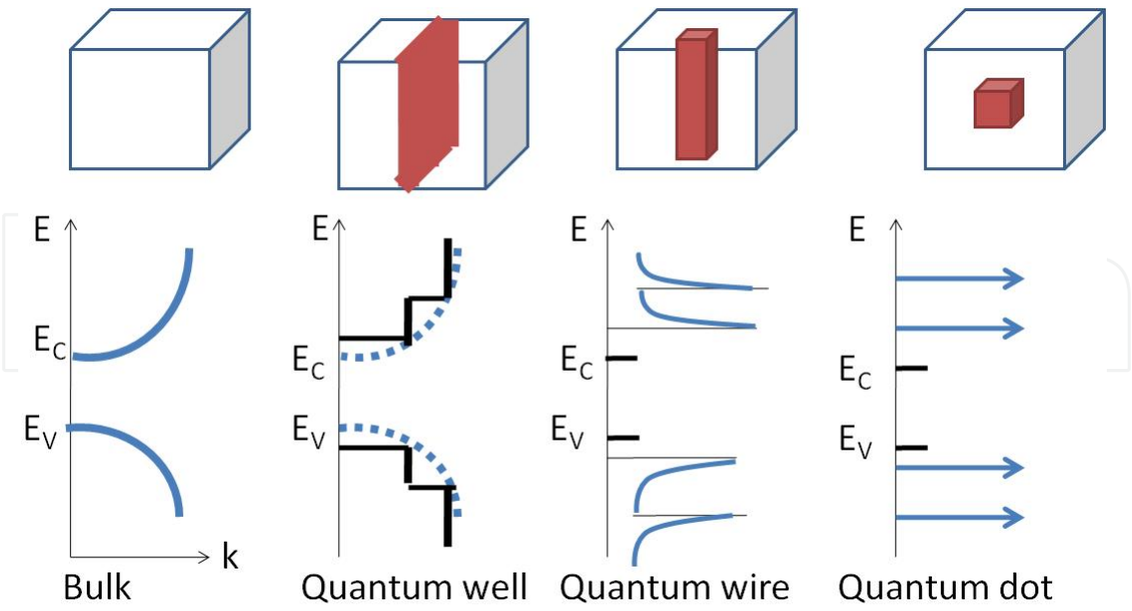

Figure 1. Schematic of density of states as system dimensionality is reduced. The density of states in different confinement configurations: (a) bulk; (b) quantum well; (c) quantum wire; (d) quantum dot. The conduction and valence bands split into overlapping subbands that become successively narrower as the electron motion is restricted in more dimensions. dimension. Adopted from [7].

In fact, quantum confinement is mainlybecause of relatively few atoms presentin a quantum dot (see Figure 2),where excitons get confined to a much smaller space, on the order of the material's exciton Bohr radius. This pronounced confinement leads to discrete, quantized energy levels more like those of an atom than the continuous bands of a bulk semiconductor. For this reason in some literatures, quantum dots have sometimes been referred to as "artificial atoms."

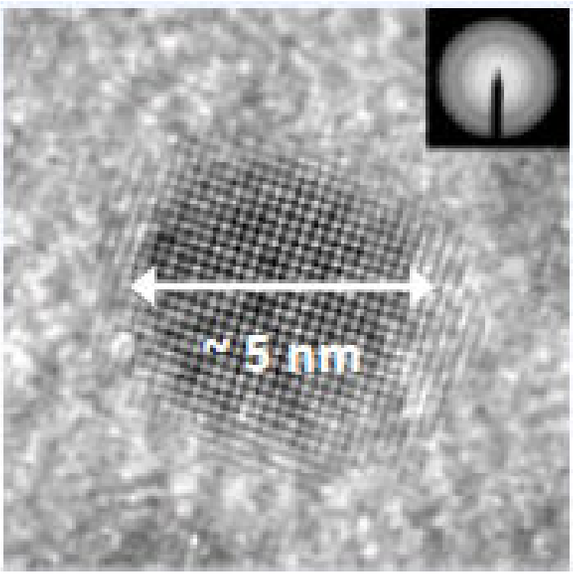

Figure 2. TEM of colloidal lead selenide PbSe quantum dot, from [8].

http://dx.doi.org/10.5772/59159

In order to specify energy eigenvalues of electrons and holes in a quantum dot, a good approximation is the infinite potential well illustrated in Figure 3. Therefore, a quantum dot can be imagined as quantum box. Assuming $\Psi_n(r)$ is the wave function of the n^{th} state. Schrödinger equation for an electron confined in one-dimensional infinite square potential well of size L is:

$$-\frac{\hbar^2}{2m}\frac{d^2\psi_n}{dx^2}+V(x)\psi_n=E_n\psi_n \tag{3}$$

The energy eigenvalues E_n and eigen-wavefunction $\Psi_n(r)$ of the Schrödinger equation are given

$$\psi_n(x)=\sqrt{\frac{2}{L}}\sin\left(\frac{n\pi}{L}x\right)+\sqrt{\frac{2}{L}}\cos\left(\frac{n\pi}{L}x\right) \tag{4}$$

$$E_n=\frac{\pi^2\hbar^2}{2mL^2}n^2,\ n=1,2,3,.... \tag{5}$$

Now if we extend the confinements of electron in three-dimensional potential well (box with dimensions L_x, L_y, and L_z) its momentum and energy will be quantized in all dimensions and we have:

$$E_{n_{x,y,z}}=\frac{\pi^2\hbar^2}{2m}\left(\frac{n_x^2}{L_x^2}+\frac{n_y^2}{L_y^2}+\frac{n_z^2}{L_z^2}\right) \tag{6}$$

With quantum dot (cubic box) of side dimension $L_x=L_y=L_z=L$,then E_n is written as:

$$E_{n_{x,y,z}}=\frac{\pi^2\hbar^2}{2mL^2}\left(n_x^2+n_y^2+n_z^2\right)=\frac{\pi^2\hbar^2}{2mL^2}n^2 \tag{7}$$

Similar energy eigenvalues can be written for holes. One must specify the m_e for electron and m_h for hole. Considering spherical shape of quantum dot with radius R, based on the effective mass model developed by Louis Brus [2] for colloidal quantum dots. The band gap E^{QD} can be approximated by:

$$E^{QD}=E_g^{bulk}+\frac{\hbar^2\pi^2}{2R^2}\left(\frac{1}{m_e}+\frac{1}{m_h}\right)-\frac{1.8e^2}{4\pi\varepsilon\varepsilon_0 R} \tag{8}$$

where ε is the relative permittivity, and $\varepsilon_0 = 8.85410^{-14}$ F.cm^{-1} the permittivity of free space.

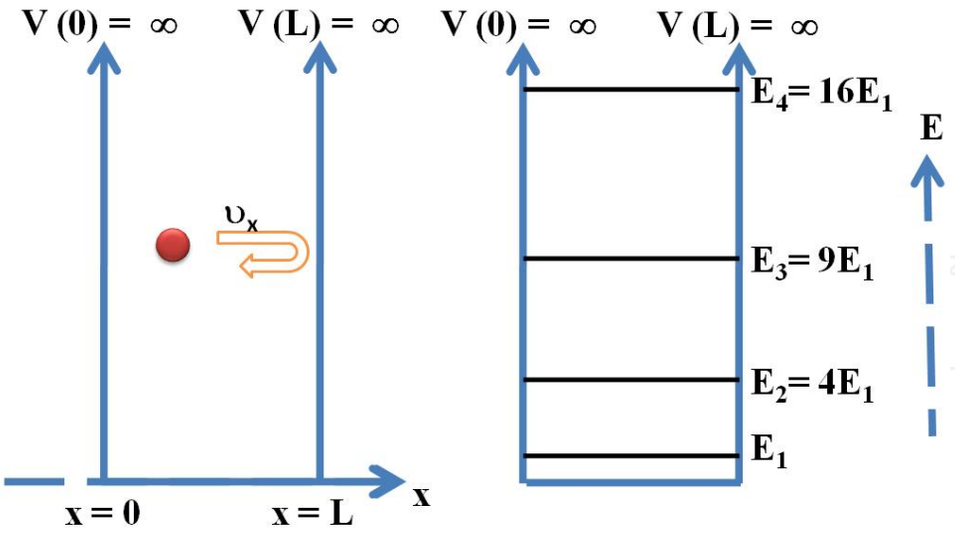

Figure 3. Infinite quantum well model.

In Equation (8), the first term on the right hand side describes the energy bandgap value of the bulk, the second term represents particle in a box quantum confinement model, and the third term details the Coulomb attraction between electron and hole (exciton). As the radius of the quantum dot decreases the Coulomb attraction term could be neglected compared to the second term in calculations. Therefore, Equation (8) indicates that bandgap energy eigenvalues increases as the quantum dot size decreases.

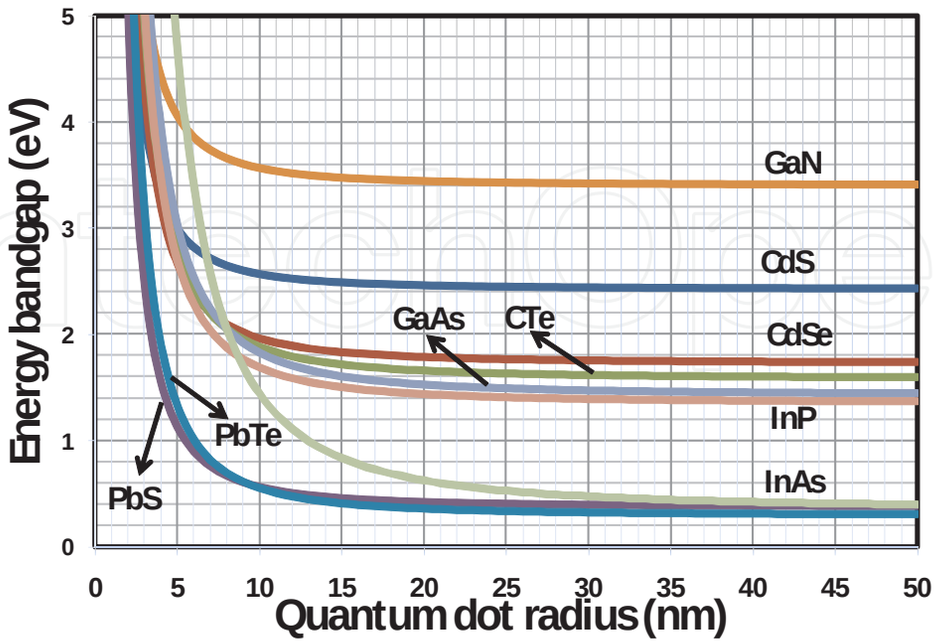

Figure 4. Variation of quantum dot energy bandgap vs. dot size for some common semiconductors. From [9].

http://dx.doi.org/10.5772/59159

Figure 4 presents few examples of well-known quantum dots, only the first and the second terms have been considered. Other detailed models such as the strong confinement model [10] have been adopted in determining the quantum dot sizes such as CdS.

Figure 5 shows the measured absorbance of three different sizes of lead sulfide (PbS) quantum dots suspended in toluene using dual beam spectrophotometer. Since a quantum dot bandgap is tunable depending on its size, the smaller the quantum dot the higher energy is required to confine excitons into its volume. Also, energy levels increase in magnitude and spread out more. Therefore, exciton characteristic peak is blue shifted.

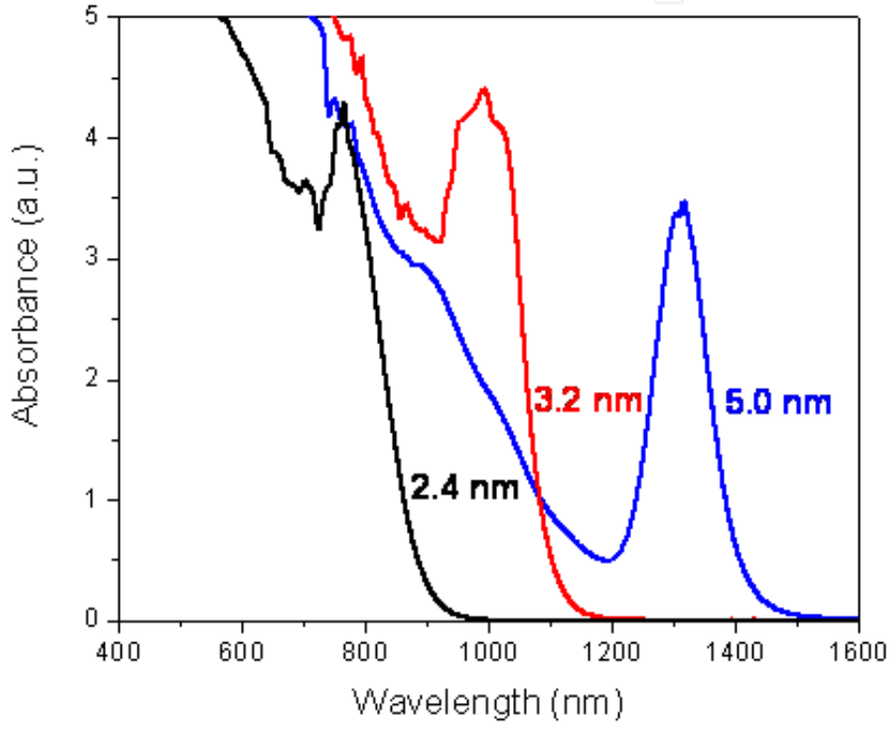

Figure 5. Measured absorbance of three different sizes PbS quantum dot suspended in toluene.

Quantum dot structured materials can be used to create the so called intermediate band. The large intrinsic dipole moments possessed by quantum dots, lead torapid charge separation.Solar cells based on intermediate bandgap materials expected to achieve maximum theoretical efficiency as high as 65%.

Nozik and his coworkwers [11-13] invesitigated Multiple exciton generation in semiconductor quantum dots. As illustrated in Figure 6, unlike bulk semiconductors such as crystalline silicon, quantum dots can generate multiple exciton (electron-hole pairs) after collisionwith one photon of energy exceeding the bandgap.In bulk semiconductor absorption of photon with energy exceeding the bandgap promotes an electron from the valance band to higher level in the conduction band these electrons are called hot carrier. The excited electron (hot carrier) undergoes many nonradiative relaxation (thermalization: multi-phonon emission) before

reaching the bottom of the conduction band. However, in a quantum dot the hot carrier undergoes impact ionization process (carrier multiplication). Therefore, absorption of a single photon generates multiple electron-hole pairs.This phenomena is called multiple exciton generation MEG. Therefore, absorption of UV photons in quantum dots produces more electrons than near infrared photons.

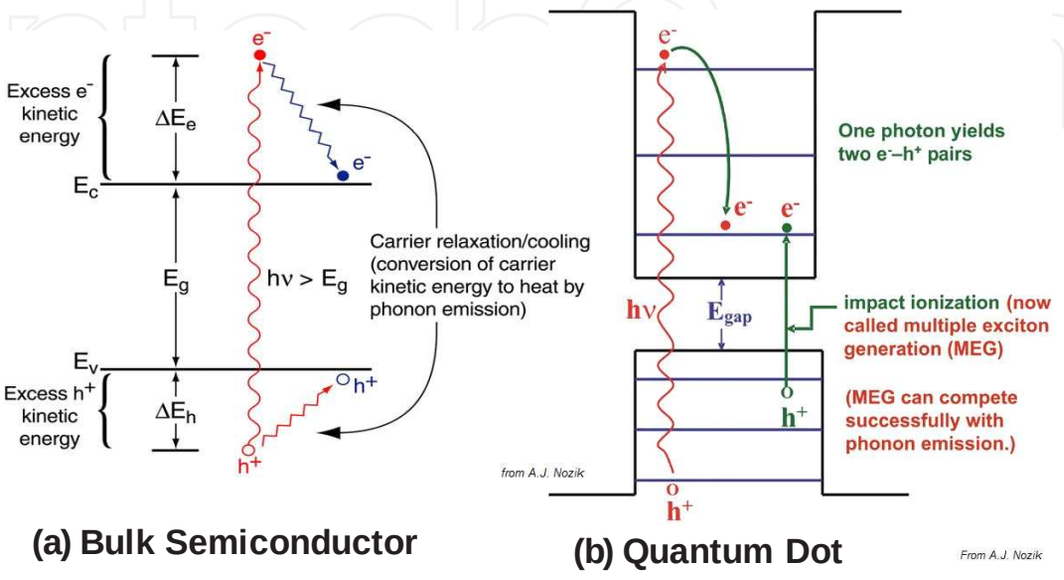

Figure 6. Thermalization of hot carriers in a bulk semiconductor (a) and a quantum dot (b), from [12].

After excitation of charge carriers the timing of the processes leading to generation of multiple charge carriers are detailed in [14] and schematically illustrated in Figure 7. After absorption of photon it takes hot carries 0.1 ps to go for impact ionization, then after 2 ps carries cool down. It takes around 20 ps for Auger recombination and finally 2ps are needed for carries to cool down and become ready for new excitation.

Experimentally carrier multiplication process-one photon generates more than one exciton via impact ionization or inverse of Auger recombination-in quantum dot has been investigated and quantified using the transient absorption spectroscopy technique. In short, [5] laser pulses are directed on the sample one for excitation and another for absorption. Measuring time of relaxation indicates whether there are single excitons recombining radiatively or biexcitons recombining via Auger recombination.

It has been discovered that there is linear proportionality between absorption change for number of generated electron-hole pairs less than 3 and number of generated electron-hole pairs. For example, investigations using PbSe and PbS QDs; confirmed 300% photo-generated carrier density (quantum yield QY)in PbSe QDs by a photon with energy of 4 times the energy spacing between the HOMO and LUMO (E_g) of the quantum dot [5, 15] as shown in Figure 8-a.Further investigations by Schaller and his coworkers [6] reported higher carrier multiplication efficiencies of 700% of photo-generated carrier density at higher photon energy to bandgap

http://dx.doi.org/10.5772/59159

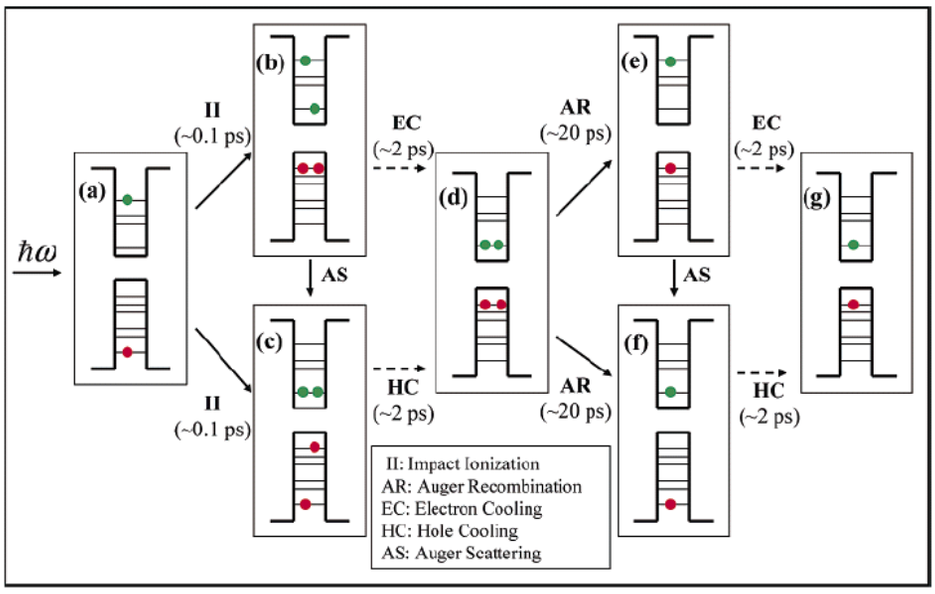

Figure 7. Illustration of the time of the processes leading to generation of multiple charge carriers in a quantum dot, from [14].

(E_g) ratios (photon energy 8×E_g).Multiplication onset starts at photon with energy equals to 3 times E_g as shown in Figure 8-b.

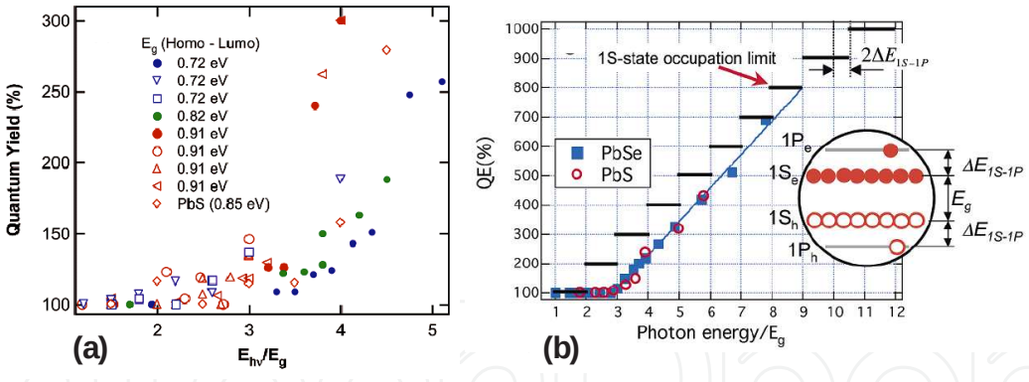

Figure 8. Experimental confirmation of carrier multiplication efficiencies. From(a) [5] and (b) [6].

4. Synthesis of quantum dots

There are many methods or techniques used in fabrication or synthesis of quantum dots that can be classified as top-down (carving large piece of a material to the desired nanostructures) or bottom-up (assembling atoms to form the desired nanostructures) methods. Generally speaking, some of these techniques are practical in solar cells applications. A summary of each synthesis method is given below.

4.1. Electron-beam lithography

Electron-beam lithography is one of the top-down methods. Electron beam system is used to etch well defined patterns on a bulk semiconductorand or superlattice, then a semiconductor layers are grown according to a well-established protocol in micro-technology.

4.2. Self-assembly growth

Self-assembly growth is one of the bottom-up methods. Molecular Beam Epitaxy (MBE) and Metal Organic Chemical Vapor Deposition (MOCVD) are widely used in the growth of the superlattice with different materials of different lattice constants.Semiconducting compound with a smaller lattice constant is grown (deposited atom by atom) on the surface of a compoundwith a larger lattice constant. The relaxation of the grown layer after specific growth thickness due to lattice mismatch results in nucleation of islands of random shapes and controllable size. This growth mode is known as Stranski-Krastanov growth (see Figure 9).MBE method, beside it is sophisticated and slow, it is expensive. However, growth control of quantum dots is precise and multi-layers of quantum dots is possible. MOCVD is used in mass production of sample wafers and in contrast to MBE the growth of crystals is by chemical reaction and not physical deposition. In this approach high vacuum and temperature are required.

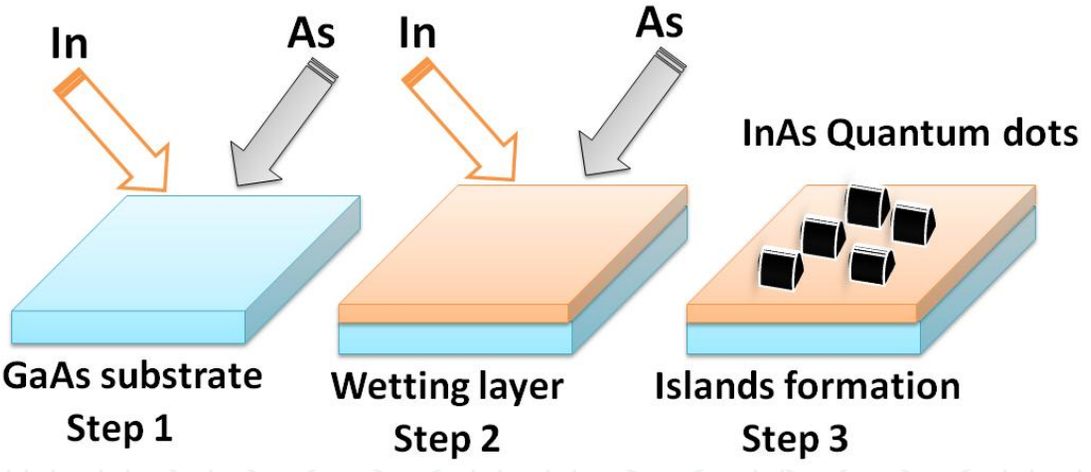

Figure 9. Schematic of InAs island formation on GaAs surface by Stranski-Krastanow growth.

4.3. Organometallic or colloidal (Wet Chemistry) synthesis method

Organometallic or colloidal (Wet Chemistry) synthesis method is one of bottom-up methods. It's also a self-assembly technique. It's relatively inexpensive and fast growth method to synthesis large quantity of quantum dots all at once. The growth could occur at non-extreme conditions. Figure 10 show a schematic of an example of the setup used in synthesis of colloidal quantum dots.

http://dx.doi.org/10.5772/59159

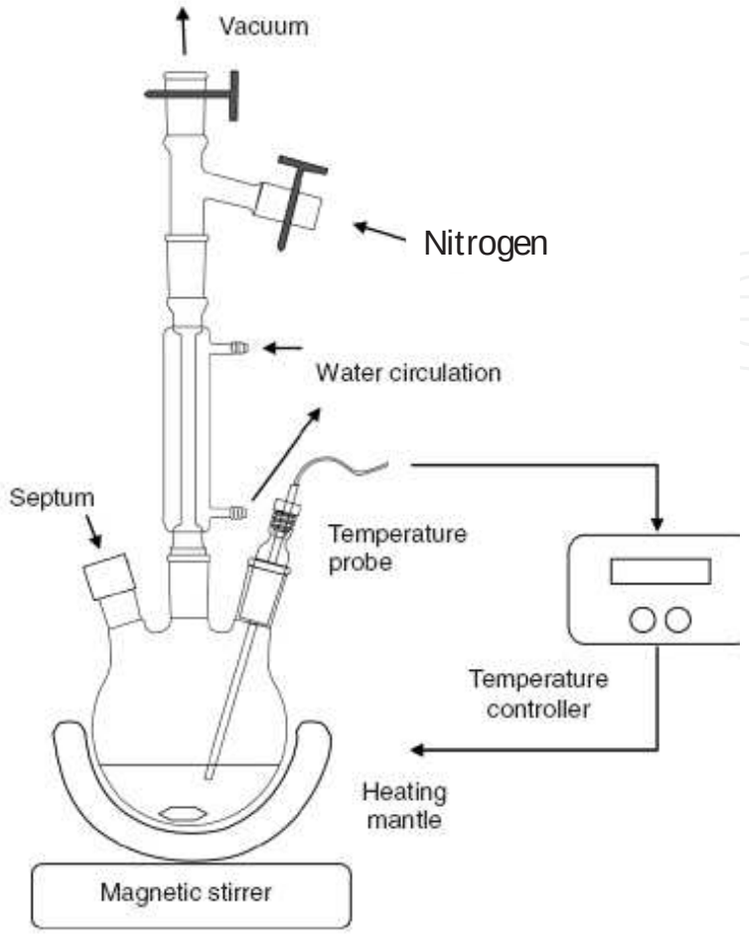

Figure 10. Schematic of a common setup used in synthesis of colloidal quantum dots.

As an example recipe given by [16] to synthesis colloidal Lead Sulfide PdS quantum dots: Heat together in a flask at 150 °C for 1 hr under N_2 flow (to make lead oleate):

- 220 mg lead(II) oxide
- 0.25 ml oleic acid (tech grade)
- 9.75 ml 1-octadecene (ODE, tech grade)

After cooling to 90-100 °C, quickly inject into the reaction flask 5 ml of 0.1 M hexamethyldisilathiane (0.5 mmol) dissolved in ODE. Then immediately cool with an ice bath.

Precipitate (methanol/butanol mixture), centrifuge and resuspend in nonpolar solvent (e.g., toluene, tetrachloroethylene, or hexanes).

$$\mathrm{PbO} + 2\mathrm{C}_{18}H_{34}O_2 - (N_2\ ODE\langle 122\ ^\circ C) \rightarrow Pb(^{et)}_{olae} + H_2O$$

$$Pb(^{et)}_{olae} + (^{i2}_{(C^{H_3}S)}S - (N_2\ ODE\langle 122\ ^\circ C) \rightarrow PbS\ quantum\ dots\ capped\ with\ \ OA$$

To manipulate functionality, alter the charge and reactivity of the surface, synthesized quantum dots usually caped with a shell from different composition. Also, the shell can enhance the stability and dispersability of the colloidal core. Magnetic, optical, or catalytic functions may be readily imparted to the dispersed colloidal core. In fact, encasing colloids in a shell of different composition may perhaps protect the core from extraneous physical and chemical changes.

Generally speaking, colloidal quantum dots could be categorized as Type-I (e.g., CdSe/ZnS) and Type-II QDs (e.g., CdTe/CdSe) as shown in Figure 11:

- In Type-I QDs, all charge carriersare confined in the core material inwhich radiative recombinationoccurs (see Figure 11-a).
- In Type-II QDs, charge carriers aresegregated in the core and shell;radiative recombination occursacross the material interface (see Figure 11-b).

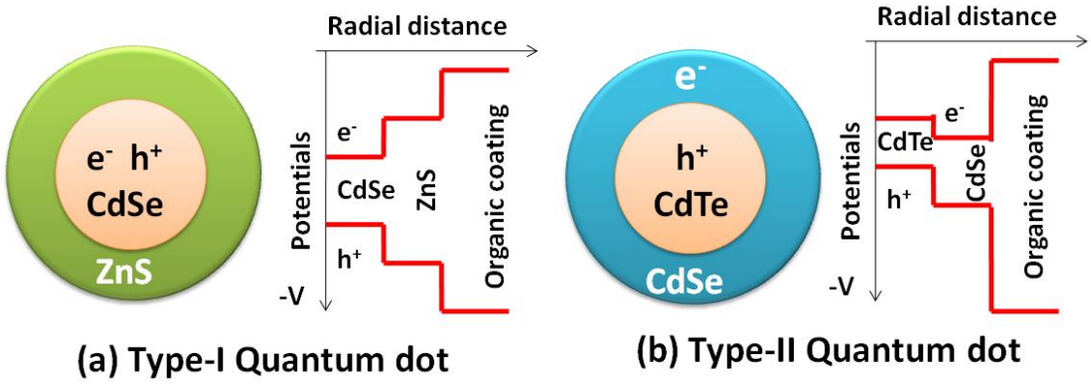

Figure 11. Illustration of (a) Type-I quantum dots (b) and Type-II quantum dots.

In fact, many researchers investigating quantum dot sensitized solar cells adopt other growth strategies to assemble quantum dots on electrode surface. We used the most direct and easiest one, the drop casting (electrode is socked with quantum dots solution drop by drop). Chemical bath deposition CBD has been used by [17], Electrophoritic deposition has been adopted by [18], successive ionic layer adsorption and reaction (SILAR) has been used by [19], and the used of bifunctional linker was demonstrated by Subramanian and coworkers [20].

5. Quantum dots solar cells

There are many realistic quantum dots based solar cells. In this section we classify them in seven strategies just as an approach to fulfill the main objective of this chapter that is introducing quantum dot solar cells. For example, [21] metal-semiconductor junction, polymer-semiconductor, and semiconductor-semiconductor systems are well know strategies of quantum dots based solar cell. Moreover; quantum dots attached to n-C_{60} composite clusters

see [18] or single and multi-walled carbon nanotubes based solar cells have been investigated [22,23].

5.1. Metal-semiconductor junction solar cell

Figure 12-a schematically shows the structure of the metal-semiconductor junctionwhich also called Schottky barrier quantum dotsbased solar cell. Itis basically fabricated from quantum dots layers (Nanocrystals film) sandwiched between metallic electrode and ITO counter electrode deposited on transparent glass substrate to act as photo-electrode.In the band diagram shown in Figure 12-b, a depletion region is due tocharge transfer to QD film. Because of high electron density in metal (~ 10^{22} cm^{-3}), the depletion is negligible on its side of the cell.

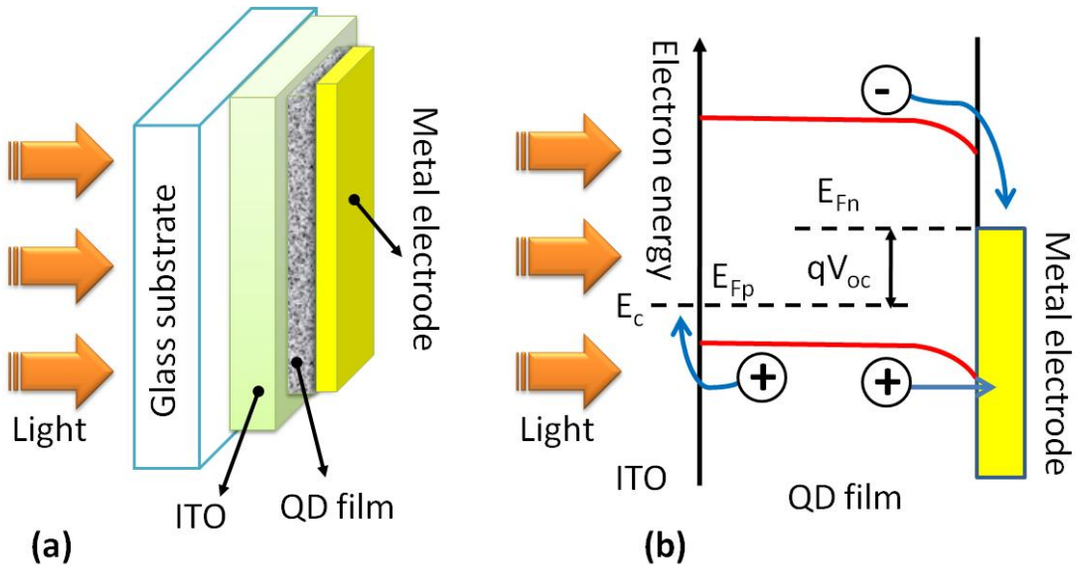

Figure 12. (a) Schematic of Schottky barrier quantum dots based solar cell, (b) band diagram of Schottky solar cell. Adopted from [24].

Layer-by-layer fabrication of quantum dots film is prepared by layer-by-layer dip coating of the substrate. For example, in layer by layer fabrication of PbSe quantum dots films, quantum dots film prepared by dip-coating, alternating between PbSe NCs in hexane and then 0.1 M EDT in anhydrous a cetonitrile, allowing the film to dry between each layer [25]. Device with 140 nm-thick QD film achieved an efficiency of ~2.2 % [26] heterojunction solar cell has been investigated by sputtering 150 nm layer of ZnO and growing layers of PbS quantum dots fabricated in air (4.1 mg/mL concentration of PbS 820 nm NC in hexanes;1 mM solution of 1,2-ethanedithiol in a cetonitrile layer-by-layer deposition for 20 cycles (~ 120nm PbS film thickness). Tested devices showed good air stability over ~1,000 hrs with cell power efficiency of 1.53 %.

It has been found [24] that the open circuit voltage in Schottky cell is constrained due to pinning of Fermi level resulted from the formed defect states at the metal-semiconductor inter-

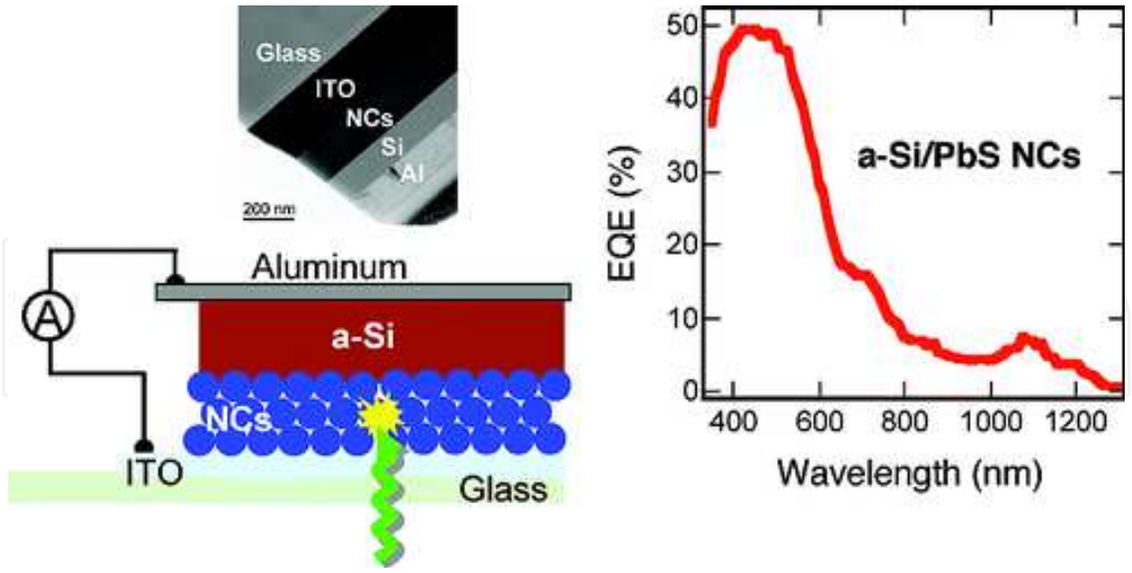

Figure 13. Hybrid silicon/PbS QD film solar cells. From [28].

face.Moreover, as illustrated in Figure 12-a, photoelectrons are firstly generated near the ITO (ohmic contact) and need to pass through long pathwayto the metallic electrode. Hence, many of the photoelectrons are encountering high recombination probability.Also on the onset of photovoltaic action the hole current injection to metallic contact is not reduce because the barrier to hole injection become less effectiveas shown in Figure 12-b. Gao J. et. al. [27] reported a method to eliminate such disadvantage by inserting a layer of a transition metal oxide (TMO) between the quantum dot (QD) layer and metal electrode. An n-Type transition metal oxide such asmolybdenum oxide (MoO_x) and vanadium oxide (V_2O_x) work as a hole extraction layer in PbS quantum dot solar cells resulted in power conversion efficiency =4.4%. The formation of dipole at the interface of MoO_x and PbS enhances the band binding and hence allowing efficient hole extraction from the PbS film valance band by the MoO_x.

5.2. Hybrid silicon/QD film (NCs) solar cells

Kilimov and his coworkers [28] demonstrated the feasibility of hybrid PV devices thatcombine advantages of mature silicon fabrication technologies with the uniqueelectronic properties of semiconductor QD (see Figure 13).The hybrid silicon/PbS QD film (Nanocrystals) solar cells show external quantum efficiencies of 7%at infrared energies and 50% in the visible and a power conversion efficiency ofup to 0.9%.

5.3. P-i-n structure solar cell

The advances in multiple quantum well solar cells [29], see Figure 14, and remarkable efficiency improvement of such p-i--n structure configurations due efficient management of photo-generated carries have encouraged researchers to replace the III-V intrinsic region of semi-conductors quantum wells structures with quantum dots.

http://dx.doi.org/10.5772/59159

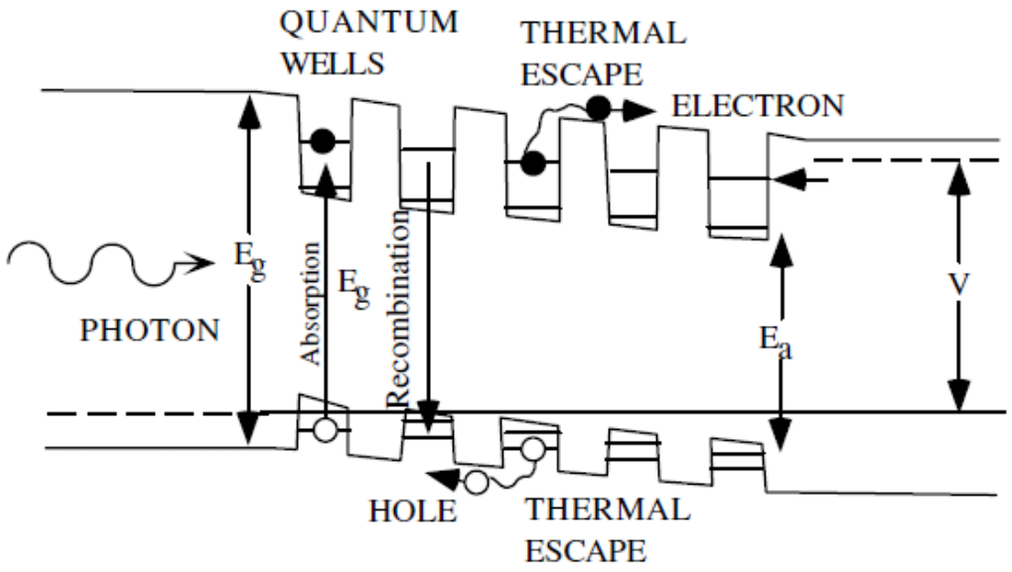

Figure 14. Multiple quantum well solar cell band structure. From [29].

Nozik and his coworkers [11,13] suggested a general p-i-n junction configuration for incorporating array of QDs into solar cells. QDs array forms the active medium of the cell (the intrinsic region). In this arrangement quantum size effects should not beeradicated due to cell architecture, excitons must be separated prior to Auger recombination, and upon absorption of photonsexcitons ought to be separated into free-charge carriers and transported to appropriate electrodes. Figure 15, shows quantum dot layers forming the i-region of a solar cell. The QDs are electronically coupled to each other to sustain electron and hole transport. Also, mini-bands are formed and hence could facilitate intermediate band formation [30]. Intermediate energy band is energy absorbing band which can accept electron excitations from the valance band and then allow transitions tothe conduction band. In quantum dots solar cells with intermediate bands photon of energies lower than the bandgap are basically absorbed and high energy photons produce hot-carries (see Figure 15). Collecting charge-carries while they are hot enhances cell voltage. On the other hand, photocurrent enhancement could be achieved by getting more from the hot-carriers via inverse Auger recombination (impact ionization) leading to multiple exciton generation MEG. One needs to bear in mind electron tunneling mechanism between quantum dots.

Investigation done by Nozik group found that [31] by comparing the performance of GaAs base solar cell to one incorporating InAs/GaAs QDs intrinsic region sandwiched between *p* and *n* GaAs emitters (grown by MBE system in the Stranski–Krastanov growth mod), the cell exhibits an extended response for photon energies lower than the GaAs bandgap. The contribution to the total current of the cell came as a result of harvesting below-bandgap-energy photons is minute (1%).

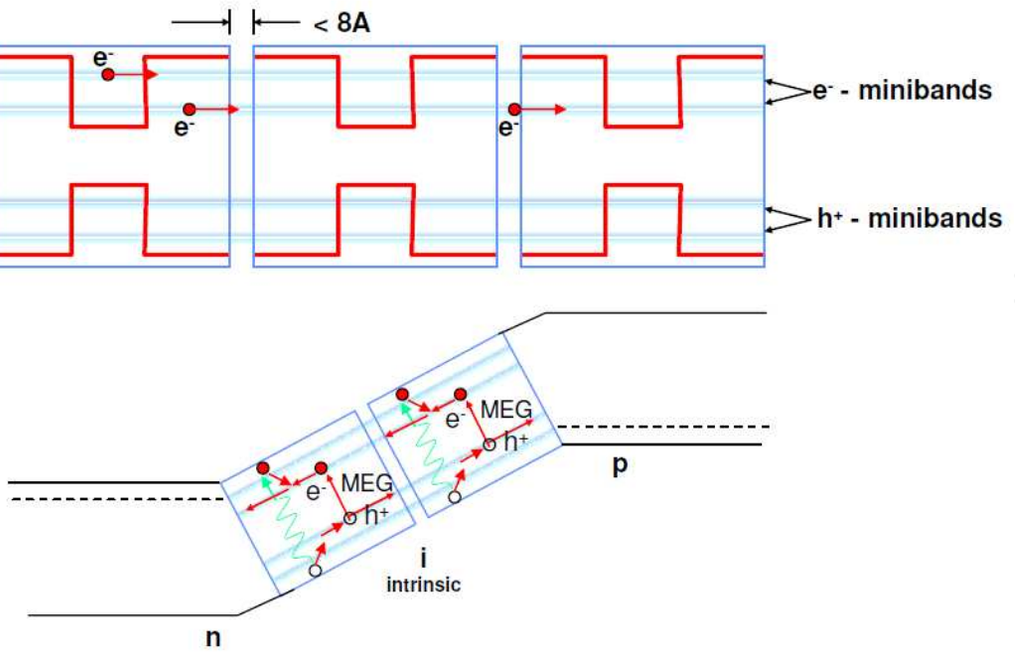

Figure 15. Possible p-i-n QD arrangements for solar cells.From [11].

5.4. Polymer-semiconductor structure configuration

In 2002 Huynh and his coworkers [32] investigated photovoltaic action in hybrid nanorods-polymer solar cells and under Air Mass (A.M.) 1.5 Global solar conditions, a power conversion efficiency of 1.7 % was obtained. This works and others encouraged many groups to investigate incorporation of quantum dots in polymers. Quantum dots are dispersed in organic-semiconductor polymer matrices. For example, in a hole-conducting polymer such as MEH-PPV (poly(2-methoxy,5-(2-ethyl)-hexyloxy-pphenylenevinylene) disordered arrays of CdSe quantum dots are synthesized. When the cell illuminated, the absorbed photons results in photo-generated carriers. As illustrated in Figure 16 [31], the photo-generated holes are injected into the MEH-PPV polymer phase which is in contact with metallic electrode to facilitate their collection.Sun et al., in 2003 reported that solar power conversion efficiencies of 1.8 % were achieved under AM1.5 illumination fora device containing 86 wt % of quantum dots [33].

5.5. Depleted heterojunction quantum dots solar cells

In depleted heterojunction colloidal quantum dot solar cells as detailed in ref. [24] a nano-structured wide bandgap semiconductor such as TiO_2 and quantum dot film are sandwiched between conductive transparent electrode (glass coated with Tin Oxide SnO_2F) and metallic (such as gold) coated electrode (see Figure 17-a).Figure 17-b illustrate the energy band diagram. Although TiO_2 has low carrier density (~10^{16} cm^{-3}) compared to metal, a depletion region in the cells forms due to charge transfer to QD film. And because of high electron density in metal (~ 10^{22} cm^{-3}), the depletion is negligible on its side of the cell. Depleted heterojunction cell overcome the disadvantages encountered with Schottky cell.

http://dx.doi.org/10.5772/59159

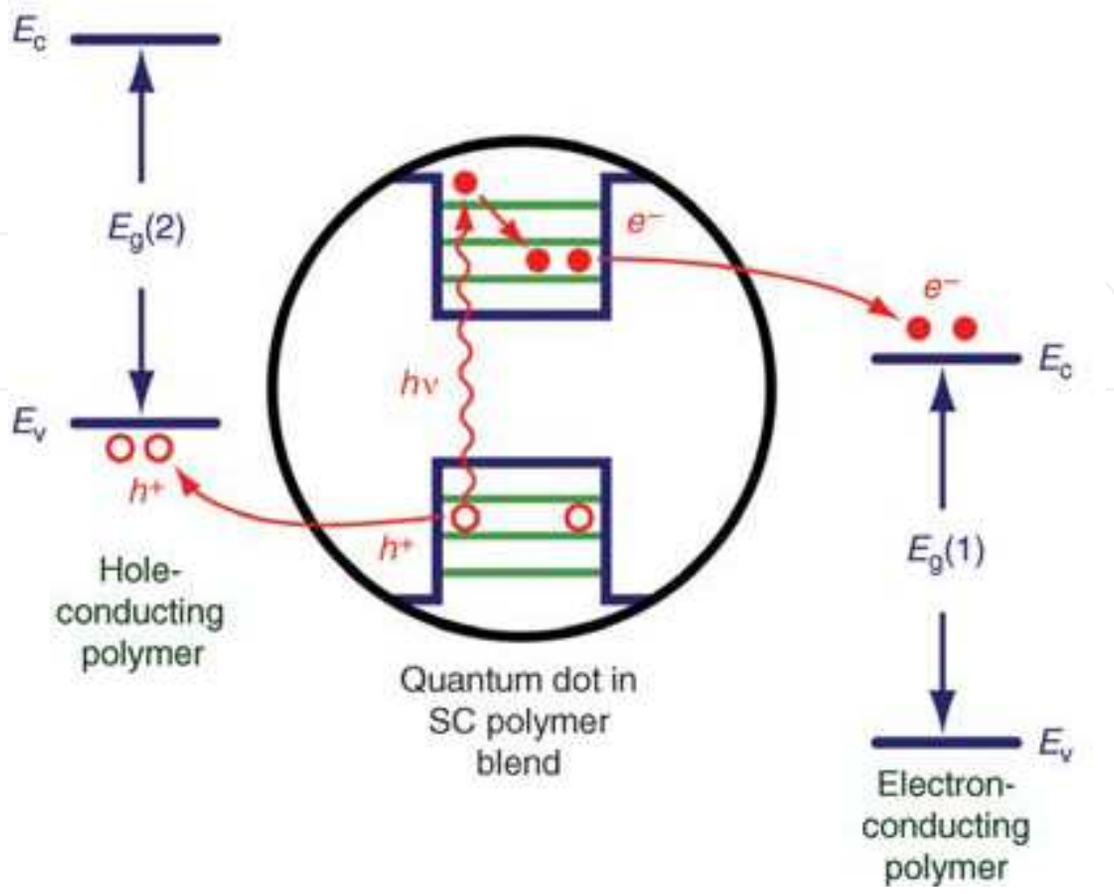

Figure 16. Shows how photo-generated carriers from quantum dots injected in conducting polymers. From [31].

In their work Grätzel and coworkers [24] have reported that the resultant depleted hetero-junction solar cells offer power conversion efficiency of 5.1% at AM1.5 illumination. The devices were capable of harvesting broadband of the solar spectrum as a result of employing infrared-bandgap size-effect-tuned PbS CQD.

5.6. Quantum dot sensitized solar cells

The structure and operation principle of QD sensitized photovoltaic cell is almost identical to dye sensitized cells [9, 34,35] with the exception that now the QDs are the source of current injection. Quantum dots can be produced in situ or more without difficulty adsorbed from a colloidal QD solution. The structure of the photovoltaic cell is shown schematically in Figure 18. In this figure, we distinguish four essential elements of the cell, namely, the conducting and counter conducting electrodes, the nanostructured TiO_2 layer, the quantum dot energy levels, and the electrolyte.

The operation of the cell can be described by the following steps and the corresponding process equations:

1. Upon absorption of a photon, a quantum dot is excited from the ground state (QD_S) to a higher energy state (QD_S^*), as illustrated by Eq.(1) below.

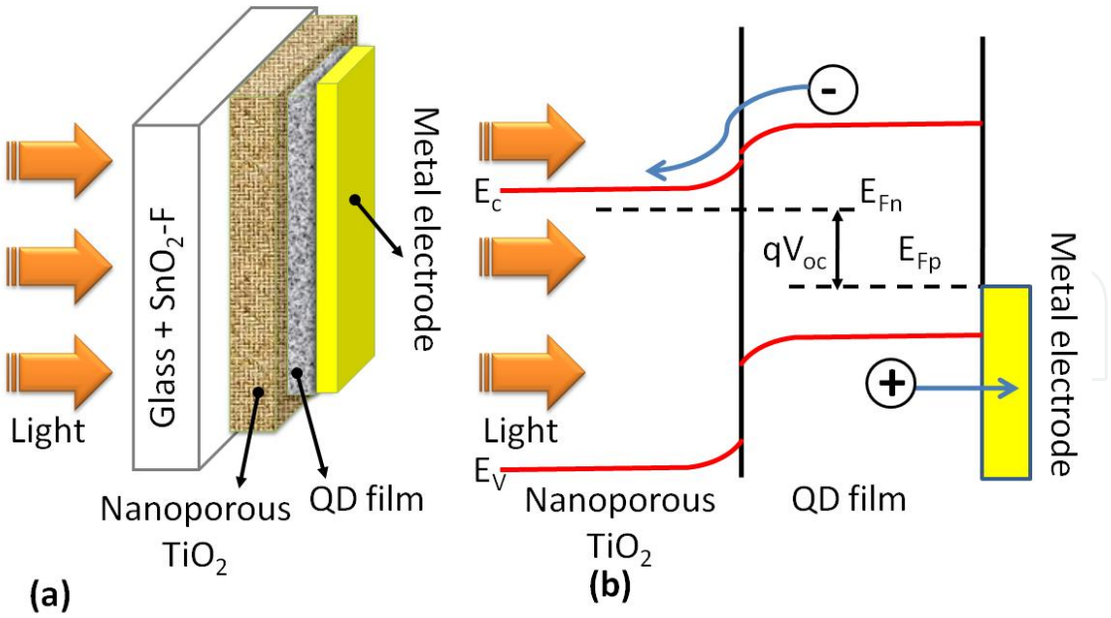

Figure 17. (a) Schematic diagram of Depleted-heterojunction Colloidal Quantum Dots Solar Cells, (b) energy band diagram. From [24].

$$\textit{Excitation process}: \mathrm{QD_S} + \mathrm{h}\,\nu \rightarrow \mathrm{QD_S^*} \tag{9}$$

Where QD_S and QD_S^* is the quantum dot in its ground state and excited state respectively.

2. The absorption process results in the creation of electron-hole pair in the form of exciton. Dissociation of the exciton occurs if the thermal energy exceeds its binding energy.

$$\textit{Exciton dissociation}: \mathrm{QD_S^*} \rightarrow \mathrm{e^{-*}} + \mathrm{h^{+*}}\left(\text{free carriers}\right) \tag{10}$$

3. The excited electron is then injected in the conduction band of the wide bandgap semiconductor nanostructured TiO_2 thin film. This process will cause the oxidation of the photosensitizer (The QDs).

$$\textit{Injection process}: \mathrm{QD_S^*} + \mathrm{TiO_2} \rightarrow \mathrm{TiO_2(e^{-*})} + \mathrm{QD_S^+} \tag{11}$$

4. The injected electron is transported between the TiO_2 nanoparticles, and then gets extracted to a load where the work done is delivered as electrical energy.

$$\textit{Energy generation}: \mathrm{TiO_2(e^{-*})} + \text{C.E.} \rightarrow \mathrm{TiO_2} + \mathrm{e^{-*}}\,(\text{C.E.}) + \text{elecrical energy} \tag{12}$$

http://dx.doi.org/10.5772/59159

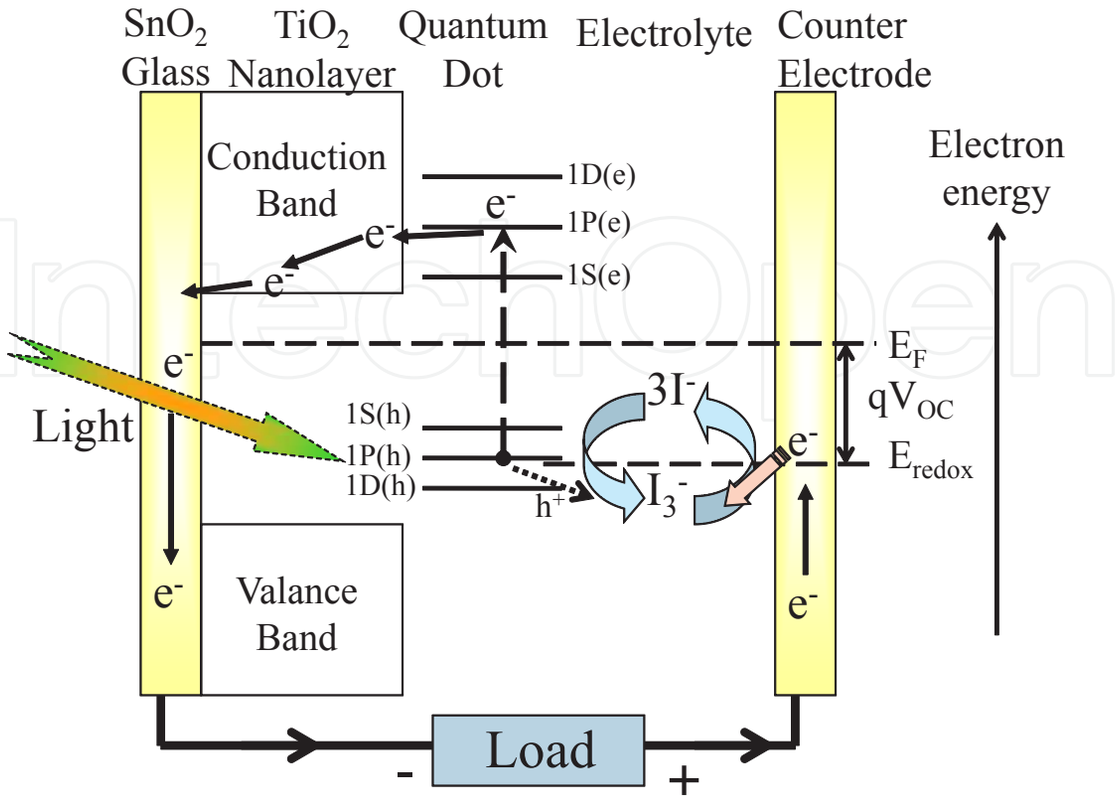

Figure 18. Schematic diagram illustrating the structure and operation of quantum dots-sensitized photovoltaic cell.

Where C.E. stands for counter electrode. The counter electrode is identical to the photoelectrode where the nanostructured TiO_2 is deposited. The counter electrode is usually coated with a catalyst (graphite).

5. Most common electrolytes used in QDSCs are aqueous polysulfide and organic electrolyte with I^-/I_3^--redox couple. In some works the liquid electrolyte has been replacedwith solid-state hole conductors such as spiro-OMeDAT andCuSCN [36]. Assuming electrolyte used in the cell contains I^-/I_3^-redox ions, that play the role of electron mediator between the TiO_2 photoelectrode and the counter electrode [9]. Therefore, the oxidized photosensitizer states (QD_S^+) are regenerated by receiving an electron from the oxidized I^-ion redox mediator, regenerating the ground state (QD_S), and I^-becomes oxidized to the oxidized state I_3^-(triodide ions).

$$Regeneration\ of\ QDs: QD_S^+ + \frac{3}{2}I^- \rightarrow QD_S + \frac{1}{2}I_3^- \tag{13}$$

6. The I_3^-diffuses to the counter electrode and substitutes the internally donated electron with that from the external load and gets reduced back to I^-ion.

$$Electron\ capture\ reaction: \frac{1}{2}I_3^- + e^-(C.E) \rightarrow \frac{3}{2}I^- + C.E. \quad (14)$$

Overall, generation of electric power in this type of cells causes no permanent chemical transformation.

To enhance electron injection into the conduction band of the TiO_2 thin film, one must choose a sensitizer with a proper matching energy gap. Quantum dots can fulfill the necessary energy gap requirement by choosing the ones with the proper size. It is interesting to note that for the QD to effectively accept the donated electron from the redox mediator. Finally, the maximum potential produced by the cell is determined by the energy separation between the electrolyte chemical potential (E_{redox}) and the Fermi level (E_F) of the TiO_2 layer, as shown in Figure 18.

The bulk of many research works done on QD synthesized solar cells focused on CdS, CdSe, and CdTe QD as sensitizers [37-39] The choice of these materials follows the success of earlier studies on identifying the morphological and electrolyte effects on their performance and stability [40-41]. Incident Photon to carriers conversion efficiency IPCE is directly related to the product of light harvesting efficiency = $1\text{-}10^{-A(\lambda)}$ (where $A(\lambda)$ is the spectral absorbance of the quantum dots sample, electron injection efficiency Φ_{inj} (how efficient are electrons injected from excited quantum dot into TiO_2 conduction band), and electron collection efficiency Φ_{coll} (how efficent are electrons are collected by the photoelectrode), hence we have:

$$IPCE = LHE \times \Phi_{inj} \times \Phi_{coll} \quad (15)$$

Light harvesting efficiency could be affected by both the type and size of quantum dots. For example PdS based quantum dots have broader spectral absorbance than CdS quantum dots. Kamat reported that charge injection from excited CdSe quantum dots into nanostructured TiO_2 film can be controlled by varying solution pH as illustrated in Figure 19 "At increasing solution pH, the conduction band of TiO_2 shifts 59 mV/pH unit to a more negative potential, thereby decreasing the driving force and thus decreasing the rate of nonradiative electron transfer from excited CdSe. The emission yield and the average emission lifetime increase with increasing pH, thus providing a way to monitor the variation in medium pH." [42].

Kongkanand and co-workers has investigated the effect of quantum dots size on charge injection rate [43]. They found that smaller-sized CdSe quantum dots show greater charge injection rates and also higher IPCE at the excitonic band.Interestingly, Larger particles have better absorption in the visible region, on the other hand,it cannot inject electrons into TiO_2 as effectivelyas smaller-sized CdSe quantum dots. It has been found that surface treatments can strongly influence charge transfer, recombination, and transport processes of photogenerated electrons and holes in QDSCs [44]. Figure 20 schematically shows that transport of electrons through the nonporous electrode is dominated by diffusion [45]. A path taken by an electron is not simply a straight line. An electron undergoes through a crisscross path before reaching

http://dx.doi.org/10.5772/59159

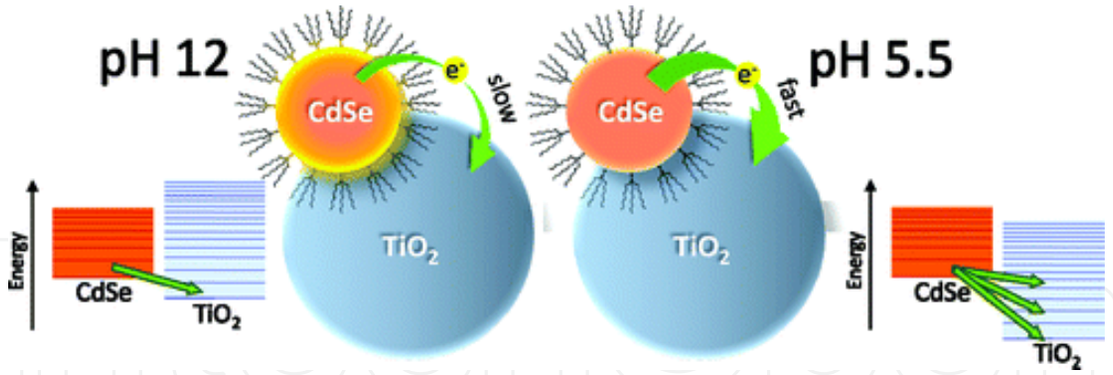

Figure 19. Illustration of how charge injection from excited CdSe quantum dots into nanostructured TiO_2 film can be controlled by varying solution pH. From [42].

the photoelectrode. The electron diffusion length, L_n is related to electron lifetime (τ_n) and diffusion coefficient (D_n) as:

$$L_n = \sqrt{D_n \tau_n} \tag{16}$$

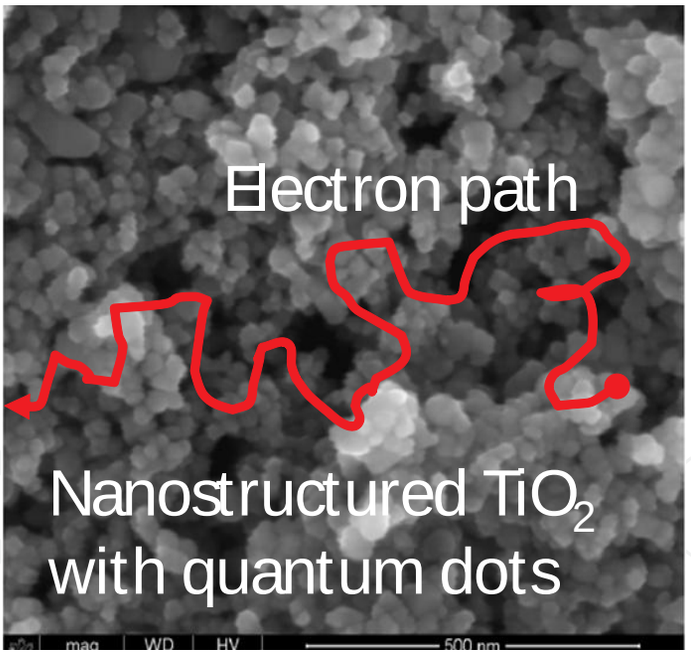

Figure 20. Illustrate a path taken by an electron after being injected into nanoporous TiO_2 layer (Not to scale). The nanoporous TiO_2 layer has been imaged using scanning electron microscope SEM.

Cell conversion efficiency is affect by morphology of the photoelectrode [43]. Tube type is more advantageous to the fast electronic conduction, due to shorter diffusion path comparedwith the particle type. For example, OTE / TiO_2 (Nanoparticles)/CdSe: 0.6 % versus Ti / TiO_2 Nanotubes /CdSe: 0.7 %.

Interesting results have been reported by some investigators who studied the incorporation of a layer of PbS quantum dots in thin film solar cells, by direct growth of PbS quantum dots on nanostructured TiO_2 electrodes [27]. Deposition of a transition metal oxide (n-type) layer on grown layer of PbS quantum dots to act as hole extractor layers [46] or employing a graded recombination layer [47].

Several methods have been employed to prepare TiO_2 thin layer. We prepared nanostructured thin films following the procedure detailed in [9, 34]. In this method, a suspension of TiO_2 is prepared by adding 9 ml of nitric acid solution of PH 3-4 (in ml increment) to 6 g of colloidal P25 TiO_2 powder in mortar and pestle. To get a white free flow-paste, we added 8 ml of distilled water (in 1 ml increment) during the grinding process. Finally, a drop of transparent surfactant is added in 1 ml of distilled water to ensure uniform coating and adhesion to the transparent conducting electrode. It was found that the ratio of the nitric acid solution to the colloidal P25 TiO_2 powder is a critical factor for cell performance. If the ratio exceeds certain threshold value, the resulting film becomes too thick and has a tendency to peel off. On the other hand, a low ratio reduces appreciably the efficiency of light generation.

Doctor blade technique was employed by depositing the TiO_2 suspension uniformly on a cleaned (rinsed with ethanol) conductive plate. The TiO_2 film was allowed to dry for few minutes and then annealed at approximately 450 °C (in a well-ventilated zone) for about 15 minutes to form a nanoporous TiO_2 layer as shown in Figure 20. The conductive plate is then allowed to cool slowly to room temperature. This is a necessary condition to remove stresses and avoid cracking of the glass or peeling off the TiO_2 layer. Once the TiO_2 nanocrystalline layer is prepared, it is coated with colloidal QDs. The counter electrode is coated with graphite that Acts as a catalyst in regenerating quantum dots. Both the photo-and counter electrodes are clamped together and drops of electrolyte are applied to fill the clamped cell. The electrolyte used is iodide electrolyte (0.5 M potassium iodide mixed with 0.05 M iodine in water free ethylene glycol) containing a redox couple (traditionally the iodide/tri-iodide I^-/I^{3-}couple). The measurements of the open circuit voltage and short circuit current have been performed under direct illumination from a solar simulator producing 1 sun illumination. UV or IR cut-off filters have been used to eliminate carrier generation from TiO_2 layer and to impede cell overheating.No antireflection coatings on the photoelectrode have been applied. Figure 21 shows an example of the obtained I-V characteristics of PdS quantum dots (size 3.2 nm) sensitized cell with power conversion efficiency =1.8 %.

As it's the case with dye sensitized solar cells, quantum dots sensitized solar cells light harvesting efficiency could be enhanced via efficient light management [48] by increasing light scattering effect [49]. The distance traveled by transmitted photons in the cell is increases by multiple scattering and hence get highly probable by the sensitizer. Surface plasmons resonance effect in the cell also has been suggested [50]. Another approach that is effective in enhancing photovoltaic effect is the reduction of the charge recombination by controlling transparent-conducting-oxide/electrolyte interface such that injected electrons in photoelectrode are excluded from recombining with the redox couple in electrolyte.

http://dx.doi.org/10.5772/59159

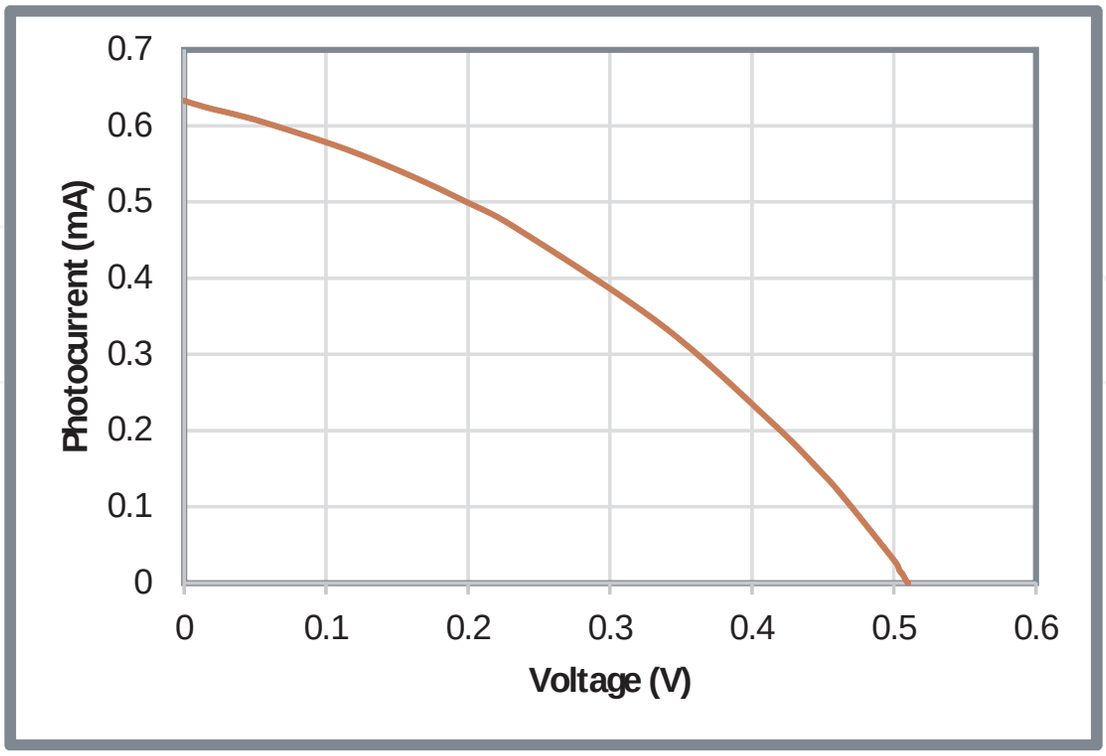

Figure 21. I-V characteristics of PbS quantum dot sensitized solar cell. Quantum dots have on the average radius of 3.2 nm.

5.7. Quantum dot-dye sensitized solar cells

Incorporation of dye with quantum dots as sensitizer of wide bandgap semiconductor has attracted attention of many research groups. For example, we found that some natural dyes are enhancing power conversion efficiency, while some others are not. Figure 22 shows an example of the I-V characteristics of a first round study of assembled cells illuminated with a collimated beam from a hot filament lamp. In cell preparation we followed the same strategy described in section 5.6 such that after coating the photoelectrode with PbS quantum dots it was soaked in dye for an hour. Then, the electrode was rinsed with deionized water and ethanol. After that the cell is assembled and tested. The dye used was extracted from a pomegranate.

New configuration based on quantum dot-dye bilayer-sensitized solar cells has been demonstrated by Zaban and co-workers [51]. The bi-sensitizer layer cell is made up of a nanocrystalline TiO_2/CdS QD+amorphous TiO_2/N719 dye. The main aim was to providea configuration having increased charge-separation efficiency by slowing the interfacial charge recombination processes that resulted in 250% increase in cell efficiency compared to a QD monolayer cell.

The configuration investigated by Zaban and co-workers [52] established on making colloidal quantum dots (CdSe/CdS/ZnS core/shell/shell quantum dots) that serve as antennas. Via nonradiative energy transfer, absorbed light is funneled to the charge separating dye molecules (SQ02 dye molecules). The colloidal quantum dot donors are incorporated into the solid TiO_2 photoelectrode resulting in high energy transfer efficiency as well assubstantial improve-

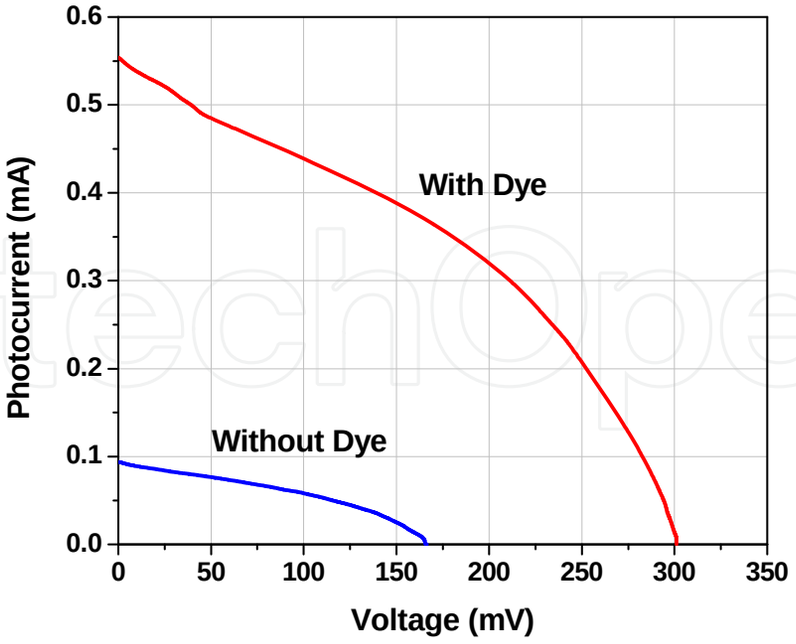

Figure 22. I-V characteristics of typical assembled quantum dot-dye sensitized solar cell. Quantum dots average size of 2.4 nm and pomegranate dye extract used as sensitizers of TiO_2 nanoporous layer.

ment of the cell stability. In this approach the processes of light absorption can be separated from charge carrier injection. Therefore, this approach enablesoptimization of each independently. Time resolved luminescence measurements relate the significant contribution of the QDs to the spectral response of the cell in the presence of the dye to Förster resonance energy transfer from the QDs to the dye molecules.

The efficiency of solar cells can be enhanced by combining quantum dots with some dye and used as a sensitizer. We suggest doing further investigations in order to understand QD-dye system. The performance of dye sensitized or quantum dots solar cells can be increased by optimizing preparation technique, using different types of electrolyte, utilizing different nanostructures (e.g., rods, stars), and replacing TiO_2 with other types of wide bandgap semiconductors such as zinc oxide ZnO.

6. Conclusion

Crystalline semiconductor solar cells besides possessing low efficiency due to their band gab limit (Shockley-Queisser limit)[53] they are expensive in terms of manufacturing cost per generated Watt of delivered electric power. In single junction bulky semiconductor solar cells, photon of energies less than the band gap are wasted since none of them are absorbed. Moreover, excess energy of those photons with energies greater than the bandgap is wasted as heat as a result of hot-carriers thermalization. A quantum dot is a crystalline semiconductor nanoparticles. Examples of well investigated quantum dots structures are CdS, CdSe, PbS, and PbSe. The operation principle of quantum dots sensitized solar cell is similar to that of the dye

sensitized solar cells DSSCs. In a quantum dot, confinement effect arises from size effect when particle size is smaller or comparable to exciton Bohr radius. As the size of the quantum dot decreases its characteristic excitonic beak get blue shifted.

Growth or synthesis methods of quantum dots are well established. In quantum dots, the rate of energy dissipation is significantly reduced, and the charge carriers are confined within a minute volume, thereby increasing their interactions and enhancing the probability for generating multiple excitons due to hot carries mechanism. There are many proposed quantum dot solar cells configurations.

The functional principle of QD-sensitized solar cell is the same as that of DSSC. The difference is that the dye in DSSC is replaced with quantum dots. This class of third generation solar cell is promising and recently attracting considerable attention. Operation principles, and performance limitations are well understood and many solutions have been proposed to enhance cell efficiency.

Acknowledgements

The author is greatly indebted to prof. Dr. Shawqi Aldallal for his kind support and encouragements. His valuable suggestions are highly appreciated. Special thanks to Miss. Fatema Aljaboori for here assistance in obtaining the I-V characteristic presented in Figure 21.

Author details

Khalil Ebrahim Jasim

Department of Physics, College of Science, University of Bahrain, Kingdom of Bahrain

References

[1] Ekimov A.I., and Onushchenko A.A. Quantum size effect in three-dimensional microscopic semiconductor crystals. JETP Lett. 1981; 34 345–349.

[2] Brus L. E. Electronic wave functions in semiconductor clusters: experiment and theory. J. Phys. Chem. 1986; 90 2555-2560.

[3] Reed M.A., Randall J.N., Aggarwal RJ, Matyi R.J., Moore T.M., and Wetsel A.E. Observation of discrete electronic states in a zero-dimensional semiconductor nanostructure. Phys Rev Lett. 1988; 60 (6) 535–537.

[4] Smith A.R., Chao K.-J., Niu Q., and Shih C.-K. Formation of atomically flat silver film on GaAs with a 'silver-mean' quasiperiodicity. Science 1996; 273 226-228.

[5] Schaller R.D., and Klimov V.I. High Efficiency Carrier Multiplication in PbSe Nanocrystals: Implications for Solar Energy Conversion. Phys. Rev. Letts 2004; 92 186601-186614.

[6] Schaller R.D., Sykora M., Pietryga J.M., and Klimov V.I. Seven Excitons at a Cost of One: Redefining the Limits for Conversion Efficiency of Photons into Charge Carriers. Nano Letters 2006; 6 424-429.

[7] Saleh, B., and Teich, M. Fundamentals of Photonics, ch.15. John Wiley & Sons, Inc. ISBNs: 0-471-83965-5 1991.

[8] Sargent E.H. Infrared Quantum Dots. Adv. Mat. 2005; 17 515-522.

[9] Jasim, K.E. Dye Sensitized Solar Cells-Working Principles, Challenges and Opportunities. In: Solar Cells-Dye-Sensitized Devices, Leonid A. Kosyachenko, (Ed),, Book Published by InTech Open Access Publisher, ISBN 978-953-307-735-2. 2011. Chapter 8, pp. 171-204.

[10] Gaponenko S.V. Strong Confinement Approximation in Optical Properties of Semiconductor Nanocrystals. New York: Cambridge University Press; 1998.

[11] Nozik, A.J. Quantum dot solar cells. Physica E 2002;14 115-120.

[12] Nozik A.J. Multiple exciton generation in semiconductor quantum dots. Chemical Physics Letters 2008; 457 3-11.

[13] Nozik A.J. Nanoscience and Nanostructures for Photovoltaics and Solar Fuels. Nano Lett. 2010; 10 2735-2741.

[14] Franceschetti A., An J.M., and Zunger A. Impact ionization can explain carrier multiplication in PbSe quantum dots. Nano Letters 2006; 6 2191-2195.

[15] Ellingson R.J., Beard M.C., Johnson J.C., Yu P., Micic O.I., Nozik A.J., Shabaev A., and Efros, Al. L. Highly Efficient Multiple Exciton Generation in Colloidal PbSe and PbS Quantum Dots. Nano Letters 2005; 5 865-871.

[16] Hines M. A., Scholes G.D. Colloidal PbS nanocrystals with size-tunable near-infrared emission: observation of post-synthesis. Adv. Mater.2003; 15 1844-1849.

[17] Yochelis S., and Hodes G. Nanocrystalline CdSe formation by direct reaction between Cd ions and selenosulfate solution. Chem Mater 2004; 16 2740-2744.

[18] Brown P. & Kamat, P.V. Quantum Dot Solar Cells.Electrophoretic Deposition of CdSe-C_{60} Composite Films and Capture of Photogenerated Electrons with nC_{60} Cluster Shell. J. Am. Chem. Soc. 2008; 130 8890-8891.

[19] Baker D.R. and Kamat P.V. Photosensitization of TiO2 Nanostructures with CdS Quantum Dots: Particulate versus Tubular Support Architectures. Adv. Funct. Mater. 2009; 19 805–811.

[20] Subramanian V, Kuno M, Kamat, V.Quantum dot solar cells. harvesting light energy with CdSe nanocrystals molecularly linked to mesoscopic TiO2 films. J Am Chem Soc 2006; 128 (7) 2385–2393.

[21] Kamat P.V. Quantum Dot Solar Cells. Semiconductor Nanocrystals as Light Harvesters. J. Phys. Chem. C 2008; 112 18737-18753.

[22] Sheeney-Haj-Kia L., Basnar B., Willner I. Efficient Generation of Photocurrents by using CdS/Carbon nanotube Assemblies on Electrodes. Angew. Chem. Int. Ed. 2005; 44 78-83.

[23] Huang Q., and Gao L. Synthesis and Characterization of CdS/multiwalled carbon nanotube heterojunctions. Nanotecnol 2004; 15 1855-1860.

[24] Pattantyus-Abraham A.G., Kramer I.J., Barkhouse A.R., Wang X., Konstantatos G., Debnath R., Levina L., Raabe I., Nazeeruddin M.K., Gratzel M., and Sargent E.H. Depleted-Heterojunction Colloidal Quantum Dot Solar Cells. ACSNano 4 (6) 3374–3380.

[25] Luther J.M., Law M.*et al.* Structural, Optical, and Electrical Properties of Self-Assembled Films of PbSe Nanocrystals Treated with 1,2-Ethanedithiol. ACS Nano. 2008; 2 271.

[26] Luther M., Gao J., Lloyd M.T., Semonin O.E., Beard M.C., and Nozik A.J. Stability... solar cell. Advanced Materials 2010; 22 (33) 3704–3707.

[27] Gao J., Perkins C.L, Luther J.M., Hanna M.C., Chen H-Yu, Semonin O.E., Nozik A.J., Ellingson R.J., and Beard, M.C. n-Type Transition Metal Oxide as a Hole Extraction Layer in PbS Quantum Dot Solar Cells. Nano Letters 2011; 11 3263

[28] Sun, B., Findikoglu A.T., Sykora M., Werder D.J., and Klimov V.I. Hybrid Photovoltaics Based on Semiconductor Nanocrystals and Amorphous Silicon. Nano Lett. 2009; 9 (3) 1235–1241.

[29] Barnham K. and Duggan G. A new approach to high efficiency multibandgap solar cells. J. Appl. Phys. 1990; 67 3490-3493.

[30] Luque A., and Marti A. Increasing the Efficiency of Ideal Solar Cells by Photon Induced Transitions at Intermediate Levels Phys. Rev. Lett. 1997; 78 5014-5017.

[31] Luque A., Martí A., and Nozik A.J. Solar Cells Based on Quantum Dots: Multiple Exciton Generation and Intermediate Bands. MRS BULLETIN 2007, 32, pp: 236-241.

[32] Huynh W.U. Hybrid Nanorod-Polymer Solar Cells. Science 2002; 295 2425.

[33] Sun B., Marx E., and Greenham, N.C. Photovoltaic Devices Using Blends of Branched CdSe Nanoparticles and Conjugated Polymers. Nano-Letters 2003; 3 (7) 961-963.

[34] Hara K., and Arakawa H. Handbook of Photovoltaic Science and Engineering, by A. Luque and S. Hegedus (Eds.), Chapter 15, p.663, John Wiley & Sons, Ltd., ISBN: 0-471-49196-9; 2003.

[35] O'Regan B.; and Grätzel M. A Low-cost High-Efficiency Solar Cell Based on Dye Sensitized Colloidal TiO_2 Films. Nature 1991; 353 737-740.

[36] Rhle S., Shalom, M., and Zaban, A. Quantum-Dot-Sensitized Solar Cells. Chem. Phys, Chem. 2010; 11 2290 –2304.

[37] Peng A., and Peng X. Formation of high-quality CdTe, CdSe, and CdS nanocrystals using CdO as precursor". Journal of the American Chemical Society 2001; 123 (1) 183–184.

[38] Lee H.J., Yum J.H., Leventis H.C. CdSe quantum dot-sensitized solar cells exceeding efficiency 1% at full-sun intensity. Journal of Physical Chemistry C. 2008; 112 (30) 11600 –11608.

[39] Bang J. H. and Kamat, P. V. Quantum dot sensitized solar cells. A tale of two semiconductor nanocrystals: CdSe and CdTe,. ACS Nano. 2009; 3 (6) 1467–1476.

[40] Wang P., Zakeeruddin S. M., Comte P., Exnar I., and Grätzel M. Gelation of Ionic Liquid-Based Electrolytes with Silica Nanoparticles for Quasi-Solid-State Dye-Sensitized Solar Cells. Chem. Commun. 2002; 24 2972-2973.

[41] Wang P., Zakeeruddin S. M., Moser J.E., Nazeeruddin M. K., Sekiguchi T., and Grätzel, M. Molecular-scale interface engineering of TiO_2 nanocrystals: Improving the efficiency and stability of dye-sensitized solar cells. Nat. Mater. 2003; 2 402.

[42] Chakrapani V., Tvrdy K., and Kamat P.V. Modulation of Electron Injection in CdSe –TiO_2 System through Medium Alkalinity", J. Am. Chem. Soc. 2010; 132 (4) 1228-1229.

[43] Kongkanand A., Tvrdy K., Takechi K., Kuno M., and Kamat P.V. Quantum Dot Solar Cells. Tuning Photoresponse through Size and Shape Control of CdSe-TiO2 Architecture. J. Am. Chem. Soc. 2008; 130 (12) 4007-4015.

[44] Mora-Sero I., and Bisquert J. Breakthroughs in the Development of Semiconductor-Sensitized Solar Cells. J. Phys. Chem. Lett. 2010; 1 3046–3052.

[45] Barnes P.R.F, Liu L., Li X., Anderson A.S., Kisserwan H., Ghaddar T.H., James R., Durrant J.S., and O'Regan, B.C. Re-evaluation of Recombination Losses in Dye-Sensitized Cells: The Failure of Dynamic Relaxation Methods to Correctly Predict Diffusion Length in Nanoporous Photoelectrodes. Nano Lett. 2009; 9 (10) 3532–3538.

[46] Braga A., Gimenez S., Concina, I., Vomiero, A., and Mora-Sero, I. Panchromatic sensities solar cells based on metal sulfied quantum dots grown directly on nanostructured TiO_2 electrode. J. Phys. Chem. Lett. 2011; 2 454-460.

[47] W X., Koleilat G.I., Tang J., Liu H., Kramer I.J., Debnath R., Brzozowski L., Barhouse D.A.R., and Levina, L.; and Hoogland, S.; Tandem colloidal quantum dot solar cells employing a graded recombination layer. Nature Photonics 2011 ; 5 480.

[48] Choi H., Nahm C., Kim J., Kim C., Kang S., Hwang T., and Park B.Toward highly efficient quantum-dot-and dye-sensitized solar cells. Current Applied Physics 2003; 13 S2-S13.

[49] Koo H.-J., Park J., Yoo B., Yoo K. Kim K., and Park N.-G. Size-dependent scattering efficiency in dye-sensitized solar cell. Inorg. Chim. Acta. 2008; 361 677-683.

[50] Atwater H.A., and Polman, A. Plasmonics for improved photovoltaic devices. Nat. Mater. 2010; 9 205-213.

[51] Shalom M., Albero J., Tachan Z., Martínez-Ferrero E., Zaban A., and Palomares E. Quantum Dot-Dye Bilayer-Sensitized Solar Cells: Breaking the Limits Imposed by the Low Absorbance of Dye Monolayers. J. Phys. Chem. Lett. 2010; 1 1134–1138.

[52] Buhbut S., Itzhakov S., Tauber E., Shalom M., Hod I., Geiger T., Garini Y., Oron D., and Zaban, A. Built-in Quantum Dot Antennas in Dye-Sensitized Solar Cells. Acs Nano 2010; 4 (3) 1293–1298.

[53] Shockley W., and Queisser H.J. Detailed Balance Limit of Efficiency of p-n Junction Solar Cells", Journal of Applied Physics 1961; 32 510-519.

IntechOpen